

# Einstein Frequency Measurement for a Strongly Coupled Dusty Plasma

Chun-Shang Wong, John Goree, *Member, IEEE*, and Zach Haralson, *Student Member, IEEE*

**Abstract**—The Einstein frequency  $\Omega_E$  was experimentally determined for a 2-D dusty plasma. We found  $\Omega_E = 49.4 \text{ s}^{-1}$  and  $50.2 \text{ s}^{-1}$  for the collection of microspheres in a crystalline and liquid-like state, respectively. Comparing to the nominal 2-D dust plasma frequency  $\omega_{pd}$ , we found the ratio  $\Omega_E/\omega_{pd} \approx 1/\sqrt{3}$ . This experimental ratio is consistent with previous predictions of Yukawa simulations. Our results were obtained by analyzing images of the microspheres to obtain their positions, charge, and the screening length; we used these measurements to calculate resonant frequencies of test particles.

**Index Terms**—2-D systems, crystal, dusty plasma, Einstein frequency, experiment, imaging, liquid, strongly coupled plasma.

## I. INTRODUCTION

IN LABORATORY experiments, dusty plasmas [1]–[3] contain micrometer-sized microspheres that are highly charged so that they exhibit strong coupling effects. As a result, the collection of microspheres can behave as a liquid [4]–[6] or as a solid-like crystalline lattice [7], [8]. The other components of a dusty plasma include weakly coupled electrons and ions, and neutral gas which apply a frictional drag on the microspheres. Video microscopy allows imaging of the microspheres, to determine their positions and velocities [9]–[11].

The most common specification for strongly coupled dusty plasmas is the Coulomb coupling parameter  $\Gamma$ . Defined as the ratio of the interparticle potential energy and thermal kinetic energy,  $\Gamma$  can be considered as a dimensionless inverse kinetic temperature [12]. A strongly coupled dusty plasma typically has solid-like behavior when  $\Gamma$  is of order  $10^3$ , and liquid-like behavior for lower values [13]. Another dimensionless parameter is  $\kappa$ , which is the ratio of the interparticle spacing and the screening length. Some dusty plasma researchers use  $\kappa$  to define an effective Coulomb coupling parameter [14]  $\Gamma_{\text{eff}}$ , which is diminished by the effects of shielding.

It is also common to specify a time scale for the motion of the microspheres in a dusty plasma, and this can be done by reporting either the dust plasma frequency  $\omega_{pd}$  or the Einstein frequency  $\Omega_E$ . A familiar practice in the dusty plasma literature is to normalize time by  $\omega_{pd}$ , and this is certainly understandable to readers from the plasma physics community; however, here we point out that the Einstein frequency will be

more easily recognized by scientists in other areas of physics. Normalizing time by  $\Omega_E$  could be especially helpful when making a physical comparison of strongly coupled plasmas with neutral liquids and solids, which of course have no plasma frequency.

The Einstein frequency can also be used to characterize how rapidly microscopic particle motion is scattered. As with molecules in a liquid, the charged particles in a strongly coupled plasma are scattered not by infrequent binary collisions, but by constant interactions with multiple neighbors, so that the researchers seldom invoke the term “collision frequency.” The concept of a collision frequency is most suitable to describe the rate of scattering by binary collisions in a weakly coupled plasma, while the rate of scattering in a strongly coupled plasma might be better described by  $\Omega_E$ .

The Einstein frequency  $\Omega_E$ , which is an abstract concept from solid-state physics [15], is a resonant frequency for the microscopic motion of a single movable atom. The neighboring atoms are assumed in this abstraction to be immovable and frozen at their equilibrium positions. This concept of an Einstein frequency for a crystal can be extended to liquids [16], although this extension requires freezing the neighboring atoms at their instantaneous positions, because unlike the case of a crystal, in a liquid the atoms have no true equilibrium positions.

In this paper, we will report an experimental determination of the Einstein frequency for the collection of microspheres in a dusty plasma, and we will compare its value to the dust plasma frequency. We will do this for both a crystal and a liquid. Although the concept of an Einstein frequency is abstract, especially because of the way it invokes immovable particles, we are able to obtain its value using instantaneous experimental data for the microsphere positions and interparticle potentials.

Previous dusty plasma researchers have devised several practical methods of obtaining the Einstein frequency [17]. These methods were developed for two simulations [14], [18] that we will discuss in the following and an experiment. In the experiment [19], individual microspheres were tracked for an extended time, to calculate their mean-square displacement. That method of estimating  $\Omega_E$  is different from the method that we use here, which is based on the positions of multiple microspheres at a single time.

## II. EINSTEIN FREQUENCY VERSUS PLASMA FREQUENCY

### A. Scale and Dimensionality

One of the conceptual differences between the plasma frequency and the Einstein frequency is the role of length scale. The plasma frequency generally describes particle motion due

Manuscript received June 23, 2017; accepted August 24, 2017. This work was supported in part by NASA, in part by NSF, and in part by the DOE. The review of this paper was arranged by Senior Editor T. Hyde. The review of this paper was arranged by Senior Editor T. Hyde. (*Corresponding author: Chun-Shang Wong.*)

The authors are with the University of Iowa, Iowa City, IA 52242 USA (e-mail: chun-shang-wong@uiowa.edu).

Color versions of one or more of the figures in this paper are available online at <http://ieeexplore.ieee.org>.

Digital Object Identifier 10.1109/TPS.2017.2746012

to charge separation at a macroscopic scale, while the Einstein frequency describes motion at a microscopic scale.

Besides scale, dimensionality of the microsphere cloud is another factor that distinguishes  $\omega_{pd}$  and  $\Omega_E$ . For dusty plasma experiments, dimensionality is of practical importance because the laboratory experiments can be done with a cloud of microspheres that either fills a 3-D volume or settles in a 2-D monolayer due to sedimentation under the force of gravity [2]. In either case, electrons and ions always fill a 3-D volume that is larger than the microsphere cloud.

The Einstein frequency is a concept that is the same in 2-D and 3-D. This is so because the microscopic restoring force in the case of a crystal is linear with small displacements, regardless of whether the microspheres lie in a 2-D plane or fill a 3-D volume. The plasma frequency, on the other hand, has a formula that must be written differently for each dimensionality.

For the case of a 3-D cloud of microspheres, the dust plasma frequency [17] formula is  $\omega_{pd} = (3Q^2/4\pi\epsilon_0ma_{3-D}^3)^{1/2}$ , and this represents a true resonant frequency exactly like an electron plasma frequency or an ion plasma frequency, for a 3-D plasma. Here  $a_{3-D} = (4\pi n_{3-D}/3)^{-1/3}$  is the 3-D Wigner–Seitz radius, while  $Q$  is the charge of the microsphere,  $m$  is the microsphere mass, and  $n_{3-D}$  is the 3-D number density of the microspheres.

For the case of a 2-D cloud [17], there is no 3-D number density for the microspheres, so it is common to write

$$\omega_{pd} = (Q^2/2\pi\epsilon_0ma_{2-D}^3)^{1/2} \quad (1)$$

where  $a_{2-D} = (\pi n_{2-D})^{-1/2}$  is the 2-D Wigner–Seitz radius and  $n_{2-D}$  is the areal number density of the microspheres. We note that (1) does not describe a true resonant frequency for microsphere motion; to understand why this is so in 2-D, one can imagine a scenario of displacing two planar sheets of charge, one consisting of dust and the other of electrons and ions. In this scenario, the restoring force arising from macroscopic electric fields would not be linearly proportional to the macroscopic displacement of the sheets as it would be for slabs in 3-D, and therefore there would be no resonant motion at this frequency. For this reason, our practice is to add the word “nominal” to the phrase “2-D dust plasma frequency” when referring to (1).

### B. Ratio

Both the plasma and Einstein frequencies arise from a combination of inertia (described by the mass  $m$  of particles), and electric forces (which depends on the charge  $Q$  and spacing  $a$  between particles). There is only one simple way to combine these three quantities ( $m$ ,  $Q$ , and  $a$ ) in a power-law expression to yield a frequency. That expression has the form  $\omega \propto Qm^{-1/2}a^{-3/2}$ . Since this form must be common to both the plasma and Einstein frequencies, we expect the ratio  $\Omega_E/\omega_{pd}$  to be a dimensionless constant. An experimental determination of this ratio is one of the goals of this paper.

The ratio of  $\Omega_E/\omega_{pd}$  is predicted by theory and simulations to be of order  $\Omega_E/\omega_{pd} = 1/\sqrt{3}$  for strongly coupled plasmas in general. This ratio is exactly  $1/\sqrt{3}$  for the special case of

a 3-D one-component plasma (OCP) [17]. For other cases,  $\Omega_E/\omega_{pd}$  can be different from  $1/\sqrt{3}$ . When shielding is added to the interactions of particles in a strongly coupled plasma (like a Yukawa OCP, for example),  $\Omega_E/\omega_{pd}$  can be somewhat diminished. Dimensionality can also affect this ratio slightly [17].

### III. EXPERIMENT

In this paper, we perform a further analysis of data from the dusty-plasma experiment of Haralson and Goree [6], [20], for the purpose of determining the Einstein frequency of the microsphere component. This experiment had microspheres that were electrically levitated in a 2-D layer within the plasma chamber. The 3-D volume of the chamber was filled with electrons and ions. The experiment was performed with several runs, for both crystalline and liquid conditions. We will compare the Einstein frequency for a crystalline run and a liquid run. For the run with liquid conditions, the experimenters applied laser heating to raise the temperature above the melting point, without changing any other parameters. This experiment, which was described in detail in [6] and [20], is briefly reviewed in the following.

A capacitively coupled plasma was generated by partially ionizing argon gas at a pressure of 6 mTorr. Radio frequency power was applied at 13.56 MHz to a lower electrode, whereas the chamber walls acted as a grounded electrode.

Approximately 6000 microspheres of 8.69- $\mu\text{m}$  diameter were introduced into the plasma. The microspheres were made of melamine formaldehyde, which is a polymer substance, and they had a mass  $m = 5.2 \times 10^{-13}$  kg, based on the manufacturer’s specifications. After the microspheres were introduced into the plasma with a simple shaker, they settled into a single horizontal layer, which was electrically levitated above the lower electrode. The microspheres were illuminated by a horizontal laser sheet and imaged from above by a top-view video camera, operated at 70 frames/s. About 1400 microspheres appeared in the camera’s field of view, which was 17.6 mm  $\times$  23.4 mm. Coordinates of microspheres were measured within each still video frame by the moment method of image analysis [9]. The typical spacing between microspheres was characterized by the 2-D Wigner–Seitz radius  $a_{2-D} = 0.307$  mm. Due to collecting electrons and ions, the microspheres accumulated a charge which was determined by a wave-spectrum method [20], [21] to have the value  $Q = -15\,500 e$ . The nominal 2-D dust plasma frequency  $\omega_{pd} = 86 \text{ s}^{-1}$  and the dimensionless screening parameter  $\kappa = 0.72$  were also obtained in the spectrum analysis. For these values, the screening length was  $\lambda = a_{2-D}/\kappa = 0.426$  mm.

In an experimental run without laser heating, the microspheres self-organized in a crystalline lattice, as seen in Fig. 1(a). For this run, the microspheres had a low kinetic temperature of about 830 K, and a large Coulomb coupling parameter  $\Gamma = Q^2/4\pi\epsilon_0a_{2-D}k_B T = 15\,400$ . (The effective Coulomb coupling parameter was  $\Gamma_{\text{eff}} = 13\,000$ , using the expression from [14].)

In the other experimental run, 12 W of laser heating was applied to melt the lattice and make a liquid. The kinetic temperature of the microspheres was increased to 98000 K,

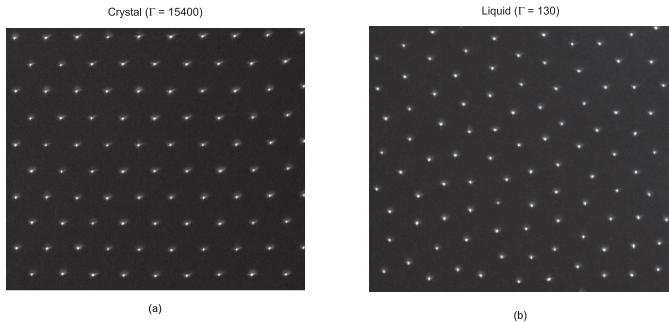


Fig. 1. Example images of microspheres in the 2-D dusty plasma. Microspheres, levitated in a horizontal monolayer, were imaged from above by a top-view video camera. We analyzed data from the camera’s entire field of view, which was  $17.6 \text{ mm} \times 23.4 \text{ mm}$ . For presentation purposes, here we show cropped images of 7% of the field of view. (a) In a run without laser heating, the microspheres self-organized into a triangular lattice, with a sufficiently low kinetic temperature so that the Coulomb coupling parameter had a large value  $\Gamma = 15400$ . (b) In a run with laser heating, the kinetic temperature of the microspheres was increased so that  $\Gamma = 130$  and the microspheres had disordered positions and behaved collectively as a liquid. Positions were measured by the moment method of image analysis [9]. In the analysis following these position measurements, we select one microsphere as a test particle and artificially assume that all other microspheres are frozen in their positions, to allow a determination of the force constant  $k$  for that test particle.

with  $\Gamma = 130$  (and  $\Gamma_{\text{eff}} = 110$ ). The microscopic spatial structure, as seen in Fig. 1(b), exhibited the disorder typical of a liquid. Other conditions, aside from the kinetic temperature and the disorder, were generally the same in the two runs.

#### IV. METHOD OF CALCULATING EINSTEIN FREQUENCY

To obtain the Einstein frequency, we obtain values for the interparticle forces, using as an input the positions of individual microspheres in a video frame. To do this requires a model for the force, which we assume to be a Yukawa (Debye–Hückel) interaction. This choice of interaction potential is experimentally justified by the binary-collision experiment of Konopka *et al.* [22]. We calculate the interparticle force as the gradient of the Yukawa potential

$$\phi(r_{ij}) = \frac{Q^2}{4\pi\epsilon_0 r_{ij}} \exp(-r_{ij}/\lambda) \quad (2)$$

for a pair of microspheres  $i$  and  $j$  separated by a distance  $r_{ij}$ . To use this expression, we require the microsphere positions, as well as values for  $Q$ ,  $m$ , and  $\lambda$ .

Before presenting our method of obtaining the Einstein frequency, we review the method that Bakshi *et al.* [18] used in their simulation. At a single time step, which is analogous to a video frame in an experiment, Bakshi *et al.* [18] artificially froze the positions of all particles, except for one test particle. The motion of their test particle was then evolved over time, taking into account forces from all the frozen particles. They Fourier analyzed the test particle’s motion, and identified the dominant frequency. This dominant frequency varied somewhat, from one test particle to another. Compiling many determinations of this dominant frequency, they prepared a histogram of its square. The mean of this histogram was compared then to the plasma frequency. For their 3-D simulation of an OCP, they found the Einstein frequency had the expected ratio of  $\Omega_E/\omega_{\text{pd}} = 1/\sqrt{3}$ .

In our analysis, we start the same way as Bakshi *et al.* [18]. Using the instantaneous particle-position data from a single video frame, we artificially froze the positions of all particles, except for one test particle. Thereafter, our procedure differed from that of Bakshi *et al.* [18]. We artificially displaced a selected test particle in a chosen direction by a small distance  $\Delta\mathbf{x}$ , which was never larger than 0.01 mm. We then computed the net force  $\mathbf{F}$  acting on the test particle, due to the other microspheres, which are analogous to the frozen particles of Bakshi *et al.* [18]. (In this force calculation, we included only the microspheres within a cutoff radius of  $6\lambda$ .) To obtain a force constant  $k$ , we made multiple displacements  $\Delta\mathbf{x}$  along the same direction, computing the net force  $\mathbf{F}$  at each displacement, and then performed a linear fit of  $\mathbf{F}$  with respect to  $\Delta\mathbf{x}$ . The slope of this fit yielded a measure of the force constant  $k$ . Next, we calculated  $\sqrt{k/m}$  to yield one observation of the resonant frequency. We repeated this process to make many more observations, first by varying the direction of the displacement  $\Delta\mathbf{x}$  over 360 angles at  $1^\circ$  intervals, and second by selecting thousands of different test particles. These calculations were repeated using a total of 102 still images from the video, to yield millions of observations.

These observations of the resonant frequency were counted to prepare histograms. These histograms are shown separately in Fig. 2(a) for the crystal run  $\Gamma = 15400$  ( $\Gamma_{\text{eff}} = 13000$ ) and Fig. 2(b) the liquid run  $\Gamma = 130$  ( $\Gamma_{\text{eff}} = 110$ ).

Our determination of the Einstein frequency is the mean of a histogram. While this result has only tiny random errors, due to our use of millions of observations, it will have a systematic error, as we discuss in the following.

#### V. RESULTS

##### A. Einstein Frequency

We find that the Einstein frequency in the experiment did not change significantly between the crystal and liquid runs. The values obtained were  $\Omega_E = 49.4 \text{ s}^{-1}$  for the crystal, and a slightly higher value of  $\Omega_E = 50.2 \text{ s}^{-1}$  for the liquid. Comparing these two results, we note a trend of  $\Omega_E$  increasing weakly with temperature, which is consistent with the simulation of Kalman *et al.* [14].

From these results, we compute the ratio of the Einstein frequency and the nominal 2-D dust plasma frequency  $\omega_{\text{pd}}$ . We find  $\Omega_E/\omega_{\text{pd}} = 0.57$  for the crystal and 0.58 for the liquid. These ratios can be also written as  $\Omega_E/\omega_{\text{pd}} = 0.993/\sqrt{3}$  and  $1.009/\sqrt{3}$ , respectively.

Next, we compare these experimental ratios to theory and simulation. As mentioned in Section II, the theory predicts  $\Omega_E/\omega_{\text{pd}} = 1/\sqrt{3}$  for a 3-D OCP. Our experiment differs from a 3-D OCP in at least two important ways: our microspheres were confined to two dimensions, and they experienced shielding. Nevertheless, we find that our experimental ratio was very close to  $1/\sqrt{3}$ .

The simulation of Kalman *et al.* [14] is more comparable to our physical system because their particles also moved in two dimensions and experienced shielding according to the Yukawa potential. They obtained  $\Omega_E$  using a formula from the quasilocalized charge approximation theory, with an input of the pair correlation function from their simulation. The ratios

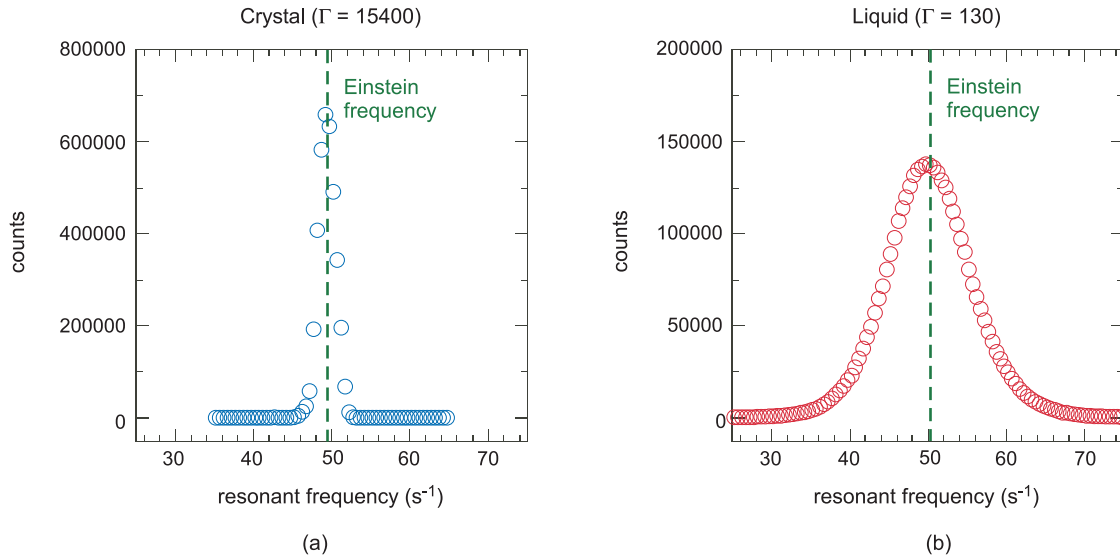


Fig. 2. Histograms of experimental determinations of the resonant frequency  $\sqrt{k/m}$ , based on the force constants  $k$  for a multitude of different test particles. Data shown here are from the same two runs as in Fig. 1. Each count in the histograms represents an evaluation of  $\sqrt{k/m}$  for a displacement of a single test particle, in a single direction, and in a single video frame. The Einstein frequency  $\Omega_E$  is obtained as the mean of the histogram, shown as dashed lines, with (a)  $\Omega_E = 49.4 \text{ s}^{-1} = 0.57 \omega_{pd}$  for the crystal and (b)  $\Omega_E = 50.2 \text{ s}^{-1} = 0.58 \omega_{pd}$  for the liquid. As compared to the crystal, the liquid has a slightly higher Einstein frequency, and its histogram has a much greater width due to the greater disorder in the positions of microspheres.

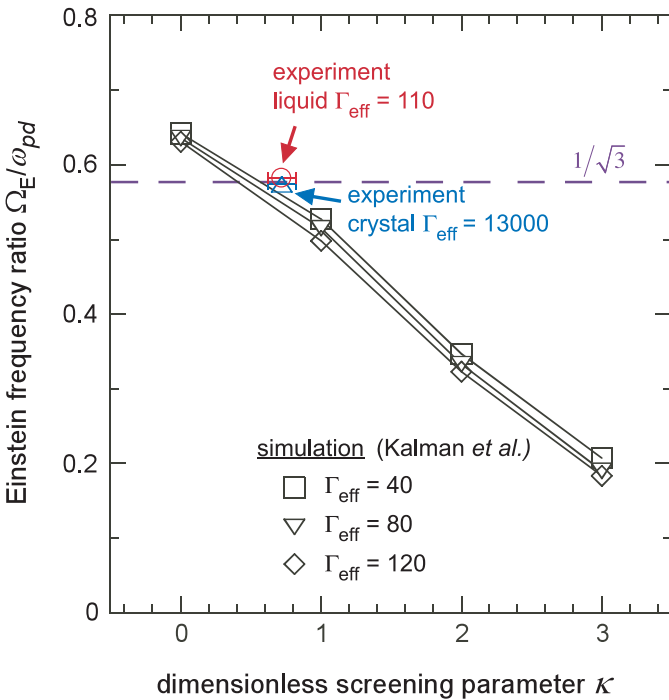


Fig. 3. Comparison of our experimentally obtained Einstein frequency  $\Omega_E$  to the simulation results of Kalman *et al.* [14]. In the vertical axis, we plot the ratio of  $\Omega_E$  to the nominal 2-D dust plasma frequency  $\omega_{pd}$ . For the horizontal axis,  $\kappa$  is the ratio of the Wigner–Seitz radius  $a_{2-D}$  to the screening length  $\lambda$ . Our experimentally obtained ratios of  $\Omega_E/\omega_{pd}$  are consistent with the simulation results, and they exhibit the same weak trend of  $\Omega_E$  increasing slightly with the dimensionless temperature  $\Gamma^{-1}$ .

of  $\Omega_E/\omega_{pd}$  reported from their simulation are plotted in Fig. 3, along with our experimental data. We see that our experimental data point for a liquid is consistent with their simulation data points, which are also for a liquid. An interpolation between the simulation data points comes to within 8% of our liquid data point.

We can also remark upon the finite width of the peaks in the histograms in Fig. 2. For a crystal, the histogram has a finite width due to at least two factors: variation of instantaneous positions of microspheres due to their finite kinetic temperature and variation of the force constant  $k$  with respect to direction in a lattice. For a liquid, the histogram is much wider, which we attribute to greater disorder in the spatial structure. A pair of microspheres in a liquid can be much closer or much farther apart than in a crystalline lattice, leading to a greater variation in the net force  $\mathbf{F}$  acting on a test particle.

### B. Measurement Errors

As mentioned above, random errors in our determination of the Einstein frequency were negligible, but systematic errors arise from uncertainties in several inputs. The two inputs that contribute the most error for our determination of  $\Omega_E$  are the values of  $\omega_{pd}$  and  $\kappa$ , which have uncertainties that were reported in [20]. We used the one-sigma range of these uncertainties to estimate the error bars in our reported values of  $\Omega_E$  as  $\pm 0.9 \text{ s}^{-1}$ , for both the crystal and liquid. Due to their systematic source, the error bars in  $\Omega_E$  for the crystal and liquid are not independent; they are either both positive or both negative, and moreover, have nearly the same magnitude. Consequently, the  $0.8 \text{ s}^{-1}$  difference between our two values of  $\Omega_E$  is statistically significant despite being smaller than the error bars.

The dimensionless ratio  $\Omega_E/\omega_{pd}$  has two principle sources of error,  $\omega_{pd}$  and  $\kappa$ . The error due to  $\omega_{pd}$  fortunately cancels, because  $\Omega_E$  and  $\omega_{pd}$  have the same dependence on  $Q$  and  $m$ . The only other input for calculating  $\omega_{pd}$  is  $a_{2-D}$ , which has a negligible uncertainty. On the other hand, the error due to  $\kappa$  does not cancel out. For our experimental data points in Fig. 3, the uncertainty in  $\kappa$  would contribute both a horizontal error bar, which we show, and a vertical error bar, which was not determined.

### C. Analytic Approximation

Separately from our experimental results, we also report an approximate analytic expression for  $\Omega_E/\omega_{pd}$ . This expression may be useful for readers of other papers that report only values of  $\omega_{pd}$ , but not  $\Omega_E$ .

We fit the simulation data points reported in Fig. 2(b) of Kalman *et al.* [14] to a simple polynomial. As compared to our experiment, their simulation has the advantage of providing results for more values of  $\Gamma$  and  $\kappa$ . We found that their data, over the ranges  $40 < \Gamma_{\text{eff}} < 120$  and  $0 < \kappa < 3$ , are fit adequately by

$$\frac{\Omega_E}{\omega_{pd}} = \frac{1}{\sqrt{3}}(1.142 - 0.00052\Gamma_{\text{eff}} - 0.225\kappa - 0.011\kappa^2). \quad (3)$$

This fit can be used with some confidence because it is good to within 5% of the simulation data points.

## VI. CONCLUSION

We experimentally determined the Einstein frequency for the microsphere component of a 2-D dusty plasma. The ratio  $\Omega_E/\omega_{pd}$  was nearly  $1/\sqrt{3}$ , which is consistent with the MD simulation of Kalman *et al.* [14]. The experimental ratio is slightly higher for liquid than for a crystal.

## REFERENCES

- [1] R. L. Merlino and J. A. Goree, "Dusty plasmas in the laboratory, industry, and space," *Phys. Today*, vol. 57, no. 7, pp. 32–38, 2004.
- [2] V. E. Fortov, A. V. Ivlev, S. A. Khrapak, A. G. Khrapak, and G. E. Morfill, "Complex (dusty) plasmas: Current status, open issues, perspectives," *Phys. Rep.*, vol. 421, pp. 1–103, Dec. 2005.
- [3] M. Bonitz, C. Henning, and D. Block, "Complex plasmas: A laboratory for strong correlations," *Rep. Prog. Phys.*, vol. 73, no. 6, May 2010, Art. no. 066501.
- [4] P. Hartmann, M. C. Sándor, A. Kovács, and Z. Donkó, "Static and dynamic shear viscosity of a single-layer complex plasma," *Phys. Rev. E, Stat. Phys. Plasmas Fluids Relat. Interdiscip. Top.*, vol. 84, no. 1, Jul. 2011, Art. no. 016404.
- [5] Y. Feng, J. Goree, and B. Liu, "Viscoelasticity of 2D liquids quantified in a dusty plasma experiment," *Phys. Rev. Lett.*, vol. 105, no. 2, Jul. 2010, Art. no. 025002.
- [6] Z. Haralson and J. Goree, "Overestimation of viscosity by the green-kubo method in a dusty plasma experiment," *Phys. Rev. Lett.*, vol. 118, no. 19, May 2017, Art. no. 195001.
- [7] C. A. Knapek, D. Samsonov, S. Zhdanov, U. Konopka, and G. E. Morfill, "Recrystallization of a 2D plasma crystal," *Phys. Rev. Lett.*, vol. 98, no. 1, Jan. 2007, Art. no. 015004.
- [8] P. Hartmann, A. Z. Kovács, A. M. Douglass, J. C. Reyes, L. S. Matthews, and T. W. Hyde, "Slow plastic creep of 2D dusty plasma solids," *Phys. Rev. Lett.*, vol. 113, no. 2, Jul. 2014, Art. no. 025002.
- [9] Y. Feng, J. Goree, and B. Liu, "Accurate particle position measurement from images," *Rev. Sci. Instrum.*, vol. 78, no. 5, May 2007, Art. no. 053704.
- [10] D. Block and A. Melzer, "Imaging diagnostics in dusty plasmas," in *Introduction to Complex Plasmas*, M. Bonitz, N. Horing, P. Ludwig, Eds. Heidelberg, Germany: Springer, 2010, pp. 135–153.
- [11] Y. Feng, J. Goree, and B. Liu, "Errors in particle tracking velocimetry with high-speed cameras," *Rev. Sci. Instrum.*, vol. 82, no. 5, May 2011, Art. no. 053707.
- [12] S. Ichimaru, "Strongly coupled plasmas: High-density classical plasmas and degenerate electron liquids," *Rev. Modern Phys.*, vol. 54, no. 4, pp. 1017–1059, 1982.
- [13] P. Hartmann, G. J. Kalman, Z. Donkó, and K. Kutasi, "Equilibrium properties and phase diagram of two-dimensional Yukawa systems," *Phys. Rev. E, Stat. Phys. Plasmas Fluids Relat. Interdiscip. Top.*, vol. 72, no. 2, Aug. 2005, Art. no. 026409.
- [14] G. Kalman, P. Hartmann, Z. Donkó, and M. Rosenberg, "Two-dimensional Yukawa liquids: Correlation and dynamics," *Phys. Rev. Lett.*, vol. 92, no. 6, 2004, Art. no. 065001.
- [15] S. H. Simon, *The Oxford Solid State Basics*. Oxford, U.K.: Oxford Univ. Press, 2013.
- [16] J.-P. Hansen and I. R. McDonald, *Theory of Simple Liquid?: With Applications to Soft Matter*. Oxford, U.K.: Elsevier, 2013.
- [17] Z. Donkó, G. J. Kalman, and P. Hartmann, "Dynamical correlations and collective excitations of Yukawa liquids," *J. Phys. Condens. Matter*, vol. 20, no. 41, 2008, Art. no. 413101.
- [18] P. Bakshi, Z. Donkó, and G. J. Kalman, "Einstein frequency distributions for strongly coupled plasmas," *Contrib. Plasma Phys.*, vol. 43, nos. 5–6, pp. 261–263, Oct. 2003.
- [19] R. A. Quinn and J. Goree, "Particle interaction measurements in a Coulomb crystal using caged-particle motion," *Phys. Rev. Lett.*, vol. 88, no. 19, Apr. 2002, Art. no. 195001.
- [20] Z. Haralson and J. Goree, "Temperature dependence of viscosity in a two-dimensional dusty plasma without the effects of shear thinning," *Phys. Plasmas*, vol. 23, no. 9, 2016, Art. no. 093703.
- [21] S. Nunomura, J. Goree, S. Hu, X. Wang, A. Bhattacharjee, and K. Avinash, "Phonon spectrum in a plasma crystal," *Phys. Rev. Lett.*, vol. 89, no. 3, 2002, Art. no. 035001.
- [22] U. Konopka, G. E. Morfill, and L. Ratke, "Measurement of the interaction potential of microspheres in the sheath of a RF discharge," *Phys. Rev. Lett.*, vol. 84, no. 5, p. 891, Jan. 2000.

Authors' photographs and biographies not available at the time of publication.